Requirements Associated with Studies into a Chain-Length Dependence of Propagation Rate Coefficients via PLP−SEC Experiments

Sabine Beuermann

Institut für Physikalische Chemie, Georg-August-Universität Göttingen, Tammannstr. 6, 37077 Göttingen, Germany

Received March 20, 2002; Revised Manuscript Received September 10, 2002

ABSTRACT: Experiments directed toward the determination of free-radical propagation rate coefficients k_p from pulsed laser initiated polymerizations (PLP) in conjunction with size-exclusion chromatography (SEC) were modeled using the program PREDICI. The simulations were carried out in order to investigate whether an experimentally observed variation of k_p with the initiating laser pulse repetition rate is necessarily due to a chain-length dependence of k_p. The modeling was performed for laser pulse repetition rates ranging from 0.5 to 50 Hz and primary radical concentrations being varied by more than 2 orders of magnitude. The resulting molecular weight distributions were very different in shape. The k_p data derived from the simulated molecular weight distributions showed a variation of about 30% with chain lengths, although the same propagation rate coefficient was introduced into all the simulations. The experimental finding of k_p being dependent on chain length induced by using different laser pulse repetition rates is not necessarily due to a chain-length dependence of k_p. The modeling results show the importance of reporting all experimental details together with k_p data derived from PLP−SEC experiments.

Introduction

More than 15 years ago it was shown that the combination of pulsed laser initiated polymerization (PLP) and polymer analysis by size-exclusion chromatography gives access to the individual propagation rate coefficient, k_p.[1] The attractiveness of the technique originates from the fact that k_p may be obtained as a quantity which is not coupled to the termination rate coefficient, k_t. In addition, k_p data are derived from a simple eq 1, which relates the number of propagation steps between two laser pulses, L_1, to the monomer concentration, c_M, and the time t_0 between two subsequent laser pulses.

$$L_1 = k_p c_M t_0 \quad (1)$$

Because of the pulsed initiation of the polymerization, a periodical change in the radical concentration with time occurs. These variations in radical concentration result in structured molecular weight distributions (MWD). A typical free-radical concentration vs time profile and a structured MWD are shown in Figure 1. Generally, L_1 in eq 1 is given by the inflection point on the low molecular weight (MW) side of the MWD and may be identified by a maximum in the derivative curve of the MWD.[1−3] For a detailed discussion of the PLP−SEC technique, the reader may for example refer to publications by an IUPAC working party on *Modeling of Polymerization Kinetics and Processes*.[4−6]

Initially, the technique was used to derive k_p data for styrene and methyl methacrylate (MMA) homopolymerizations.[1] The k_p values obtained by different laboratories agree very well with each other.[4,6] This is important considering the enormous scattering of k_p data published previously, which is reflected in the k_p data collected in the *Polymer Handbook*.[7] The PLP−SEC investigations were extended to homopolymerizations of a large number of monomers in bulk as well as in solution or in heterogeneous phase reactions. In addition, k_p values were determined in copolymerizations (for original references see e.g. two recent reviews[8,9]).

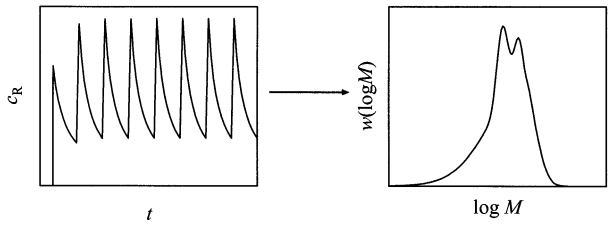

Figure 1. Schematic representation of a radical concentration−time profile (left) occurring in pulsed laser initiated polymerizations and resulting molecular weight distribution (right).

The literature demonstrates that PLP−SEC is a powerful tool not only for determining individual k_p data but also for studying additional aspects of the propagation reaction, e.g., the solvent influence on k_p or the determination of monomer concentrations in compartmentalized systems. Some studies showed that k_p may increase slightly in a few systems when the laser pulse repetition rate is increased.[10] The reason was not clear. Equation 1 indicates that the number of propagation steps (i.e., the radical chain length reached) between two laser pulses is directly correlated to the time between two successive laser pulses. Thus, it may seem obvious to explain a variation in k_p with the laser pulse repetition rate with a chain-length dependence of k_p. Recently, PLP−SEC experiments have been reported in which the laser pulse repetition rate was varied over a wide range.[11,12] The data presented by Olaj and coworkers indicate that k_p values change by about 25−30%. This is demonstrated in Figure 2, which gives the variation of k_p with chain length calculated according to eq 6b and the parameters given in Table 4 of ref 11. It was concluded that this change in k_p reflects the chain-length dependence of the propagation rate. This finding was surprising, because it had generally been accepted that the rate coefficient for the chemically controlled reaction between a radical and a molecule of low molecular weight is independent of the radical chain length.[13,14] Exceptions are the initial propagation steps

10.1021/ma020437m CCC: $22.00
Published on Web 11/01/2002

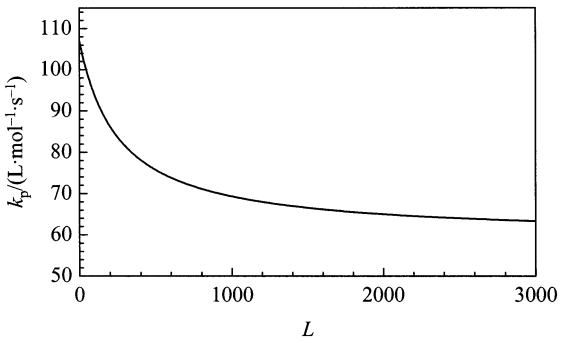

Figure 2. Apparent variation of the experimentally determined propagation rate coefficient k_p with chain length L as reported by Olaj et al. in ref 11. The curve is calculated according to eq 6b and the parameters given in Table 4 of ref 11.

up to a chain length of three or four, in which the k_p values are higher than for the reactions of longer radicals.[15,16]

In the publication by Olaj and co-workers,[11] one example for a molecular weight distribution (MWD) derived from PLP with a laser pulse repetition rate of 2 Hz is given. The MWD shows a clear PLP structure, and a k_p value of 81.9 L mol^{-1} s^{-1} is calculated according to eq 1 from the first inflection point of the GPC trace. This value for k_p agrees well with previously published data, which also used low laser pulse repetition rates. However, the paper does not contain MWDs that were obtained from PLP at a high laser pulse repetition rates, ν_{rep}, and resulted in higher k_p values. Other publications on k_p determination via PLP−SEC showed that very different shapes of the polymer MWD generated by PLP may be obtained for a given monomer depending on the reaction conditions.[10,17] In the absence of significant chain transfer (as in styrene and methacrylate polymerizations), the shape of the distribution is controlled by ν_{rep} and the termination rate. The latter depends on the termination rate coefficient k_t and the radical concentration. The influence of the termination rate on the shape of the MWD and on the determination of k_p has already been discussed for example by Hutchinson et al.,[18] Schweer et al.,[2] and Buback et al.[3]

This publication tests whether a variation of k_p by 30% induced by applying widely varying laser pulse repetition rates is necessarily due to a chain length dependence of k_p. PLP experiments were modeled using the program PREDICI. The modeling was carried out applying a constant k_p value for all laser pulse repetition rates. The calculations were performed with rate coefficients typical of styrene bulk polymerizations.

Modeling of Free-Radical Polymerizations

The shape of the MWD is determined by several rate coefficients, the concentration of primary initiator derived radicals c_R^0 and time t_0, which is given by $t_0 = \nu_{rep}^{-1}$, where ν_{rep} is the laser pulse repetition rate. Molecular weight distributions are obtained from modeling of free-radical polymerizations using the program PREDICI. The modeling is based on the following simplified reaction scheme:

$$\text{initiation:} \quad R_{Ini} + M \xrightarrow{k_I} R_1$$

$$\text{propagation:} \quad R_n + M \xrightarrow{k_p} R_{n+1}$$

$$\text{termination:} \quad R_n + R_m \xrightarrow{k_t} P_{n+m}$$

$$\text{chain transfer to monomer:} \quad R_n + M \xrightarrow{k_{tr,M}} P_n + R_1$$

where R_{Ini} is an initiator-derived primary radical, R_1 is a small radical with one monomeric unit at the chain end, R_n a radical of chain length n, M the monomer, and P_n the polymer of chain length n. The rate coefficients for propagation, termination, and chain transfer to monomer are k_p, k_t, and k_{tr}, respectively. The simulations were carried out for primary radical concentrations c_R^0 generated by each laser pulse ranging from 1×10^{-5} to 1×10^{-9} mol L^{-1}. The laser pulse repetition rates were varied between 0.1 and 50 Hz.

The simulations are based on the assumption that the initiator-derived radicals R_{Ini} form instantaneously compared to the subsequent reaction steps of the R_{Ini} radicals. The kinetic coefficients are $k_I = 200$ L mol^{-1} s^{-1}, $k_p = 75$ L mol^{-1} s^{-1}, $k_t = 5 \times 10^7$ L mol^{-1} s^{-1}, and $k_{tr} = 4.35 \times 10^{-3}$ L mol^{-1} s^{-1}. The monomer concentration in all simulations was 8.5 mol L^{-1}. The termination reaction is considered to proceed via combination only. However, the mode of termination does not significantly influence the k_p determined from simulated MWDs.[3] This assumption should not affect the modeling results from this work, since the only parameters varied in the simulations are the laser pulse repetition rate and the initial free-radical concentration c_R^0 generated by each laser pulse. Both quantities are not expected to change the ratio of combination to disproportionation.

The simulations were carried out for 13 pulses in total. The MWDs discussed in this work refer to polymer produced exclusively between the 12th and 13th pulse. The polymer generated up to the irradiation by the 12th pulse was deleted, while the complete radical distribution is taken into account for modeling the MWD between pulses 12 and 13. This procedure allows for a time efficient calculation of a polymer MWD that represents material produced at low conversion under pseudostationary conditions. The next sections consider the chain-length distribution $w(\log L)-\log L$ (CLD) instead of the MWD. CLDs are chosen, because the calculation of k_p according to eq 1 considers the characteristic chain length L_1. This procedure may be questionable only for simulations of polymerizations with high ν_{rep} and low c_R^0, since they require a higher number of laser pulses to establish a pseudostationary radical concentration vs time profile. Thus, for ν_{rep} of 25 and 40 Hz and a primary radical concentration of $c_R^0 = 1 \times 10^{-7}$ mol L^{-1} the polymer MWDs produced between the 24th and the 25th pulse were calculated as well. The distributions agree well with distributions calculated between the 12th and the 13th pulse.

Results and Discussion

Variation of ν_{rep} at a Constant Primary Radical Concentration c_R^0. *Shape of the Chain Length Distribution*. The chain-length distributions were calculated for a radical concentration of $c_R^0 = 1 \times 10^{-7}$ mol L^{-1} generated by a single laser pulse. The pulse repetition rates were varied from 0.1 to 50 Hz. A structured CLD was obtained for laser pulse repetition rates between 0.5 and 33 Hz. Figure 3 shows CLDs (full lines) obtained for repetition rates of 0.5, 1, 2, 5, 10, and 25 Hz. The shape of the CLDs is significantly different for the

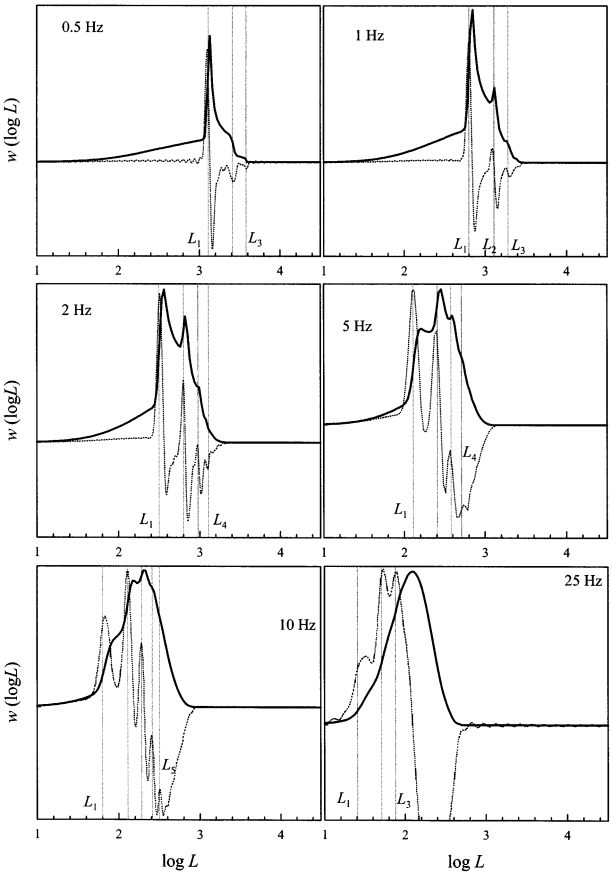

Figure 3. Chain length distributions (bold line) obtained from PREDICI simulations with $c_R^0 = 1 \times 10^{-7}$ mol L^{-1} and laser pulse repetition rates as indicated; dotted lines show the corresponding first-derivative curves, and the vertical lines indicate expected positions of the maxima of the derivative curves.

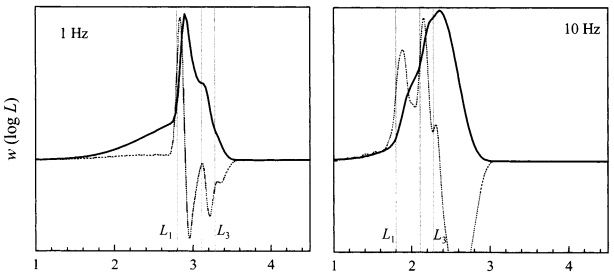

Figure 4. Chain length distributions (bold lines) for ν_{rep} of 1 and 10 Hz shown in Figure 3 after applying the broadening procedure (see text) with $\sigma_v b = 0.04$; dotted lines give corresponding first-derivative curves, and vertical lines indicate expected positions of the maxima of the derivative curves.

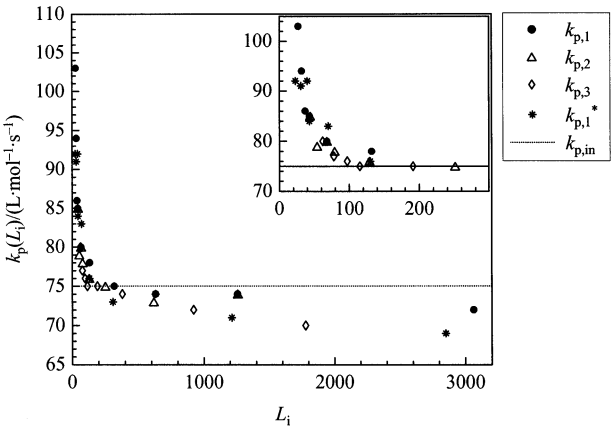

Figure 5. Propagation rate coefficients $k_p(L_i)$ as a function of the chain length of the ith inflection point used to calculate k_p. $k_{p,1}$* is obtained from the posititon of the first inflection point after applying the broadening procedure with $\sigma_v b = 0.04$. $k_{p,in}$ indicates the k_p value of 75 L mol^{-1} s^{-1} used in the simulations.

repetition rates applied. Repetition rates between 1 and 10 Hz result in distributions with several peaks. The highest repetition rate of 25 Hz produces a broad, almost structure-less, monomodal peak. With increasing ν_{rep} the size of the first peak decreases, and the second and third peak become more distinct. At 10 Hz the third peak is the most pronounced. The dotted lines in Figure 3 represent the first derivative of the CLD. In all cases at least three maxima are seen in the derivative curve, indicating the inflection points of the CLDs. For intermediate repetition rates between 2 and 10 Hz four or five inflection points occur. The vertical lines in Figure 3 mark the theoretical positions of the inflection points L_i calculated from the k_p value introduced into the modeling ($k_{p,in}$) according to $L_i = ik_pc_Mt_0$, with i indicating the 1st, 2nd, ..., 5th inflection point. For ν_{rep} ranging from 1 to 5 Hz the positions of the maxima of the derivative curves agree very well with the theoretical predictions. CLDs obtained at 10 and 25 Hz are fairly broad. Because of the short time interval between two subsequent pulses, the termination probability is reduced, and thus the peaks in the CLD at higher molecular weights are more pronounced. The derivative curves show first maxima at molecular weights higher than predicted.

The CLDs originating from modeling given in Figure 3, especially at 1 and 2 Hz, show very sharp distinct peaks, which are not seen in experimentally derived distributions. This is mainly due to the axial dispersion in SEC analyses. To compare experimental and theoretical distributions, the latter were treated applying a broadening procedure described by Buback et al. in detail.[3] In the present work distributions are broadened with a broadening constant $\sigma_v b = 0.04$. This value represents a modest axial dispersion in SEC analysis. As an example, Figure 4 shows the simulated CLDs for 1 and 10 Hz after applying the broadening procedure. The distributions are less structured with only one peak with several shoulders. The first-derivative plots represented by the dotted line exhibit three distinct maxima at the three inflection points of the CLDs. At 1 Hz these maxima again agree very well with the theoretical value included as vertical lines. However, at 10 Hz the discrepancy between the actual maximum position after broadening and prediction is 10.7%.

Calculation of k_p. The derivative curves for laser pulse repetition rates between 0.5 and 33.3 Hz have three or more maxima. At 0.2 Hz the derivative shows one distinct maximum and a shoulder at around twice the chain length of L_1. Thus, k_p values are only calculated from L_1. The values of $k_p(L_i)$ for CLDs without broadening are plotted as a function of the chain length L_i in Figure 5 and are listed in Table 1. The k_p values calculated from characteristic chain length L_i of at least 200 are almost constant for all L_i. The constant k_p at high chain length agrees well with the $k_{p,in}$ of 75 L mol^{-1} s^{-1} used in the simulation (given by the dotted line). The inset shows an expansion of the plot for chain lengths up to 300. It indicates an increase of k_p by up to 27% for chain lengths below 100.

Table 1. k_p Data and Positions of the Point of Inflection for Different Laser Pulse Repetition Rates ν_{rep} Derived from Chain-Length Distributions Obtained via PREDICI Simulation with $c_R^0 = 10^{-7}$ L mol^{-1} s^{-1} and All Kinetic Coefficients Kept Constant[a]

ν_{rep}/Hz	L_1	k_{p1}	L_2	k_{p2}	L_3	k_{p3}	L_4	k_{p4}	L_1*	k_{p1}*	N_{poi}*
0.2	3062	72							2850	69	2
0.5	1257	74							1213	71	2
1	632	74	1260	74	1778	70			631	74	3
2	318	75	618	73	921	72			308	73	3
5[b]	132	78	251	75	380	74	501	74	130	76	4
10[c]	68	80	129	76	191	75	251	74	70	83	3
16.6	43	85	79	78	115	75	151	75	43	84	2
20	37	86	68	80	97	76	126	74	40	92	2
25	32	94	54	79	79	77			31	91	2
33.3	27	103	44	85	62	80	76	74	24	92	2

[a] L_1* and k_{p1}* were derived from the first inflection point of CLDs after applying the broadening procedure with $\sigma_v b = 0.04$. N_{poi}* gives the number of inflection points of the CLD after broadening. [b] Also a fifth and a sixth inflection point occurring. [c] Also a fifth inflection point occurring; all k_p data in units of L mol^{-1} s^{-1}.

Table 2. k_p Data Derived from CLDs Obtained via PREDICI Simulation for Laser Pulse Repetition Rates of 0.5 and 25 Hz with All Kinetic Coefficients Being Kept Constant; For Further Details See Text[a]

0.5 Hz	$\sigma_{vb} = 0$		$\sigma_{vb} = 0.04$		25 Hz	$\sigma_{vb} = 0$		$\sigma_{vb} = 0.04$	
c_R^0 /mol L^{-1}	L_1	k_{p1}	L_1	k_{p1}	c_R^0 /mol L^{-1}	L_1	k_{p1}	L_1	k_{p1}
5×10^{-9}	1245	73	1247	73	1×10^{-7}	32	94	sh	
1×10^{-8}	1291	76	1247	73	5×10^{-7}	28	83	25	72
2×10^{-8}	1330	78	1244	73	1×10^{-6}	28	81	26	75
5×10^{-8}	1288	76	1211	71	2×10^{-6}	26	77	25	73
7×10^{-8}	1259	74	1169	69	4×10^{-6}	28	83	25	74
9×10^{-8}	1247	73	1188	70	5×10^{-6}	25	73	24	71
1×10^{-7}	1257	74	1175	69	5×10^{-6}	25	73	23	68
2×10^{-7}	1274	75	1153	68	7×10^{-6}	25	73	25	73
3×10^{-7}	1245	73	1183	70	9×10^{-6}	25	74	25	73
4×10^{-7}	1271	75	sh		1×10^{-5}	24	70	24	70

[a] All k_p values in units of L mol^{-1} s^{-1}. sh = shoulder on the high molecular weight side of the CLD.

In addition, Figure 5 and Table 1 contain k_p values derived from L_1 of the CLDs after broadening. These k_p values are also independent of the chain length at high values of L_1. For shorter chain lengths, k_p increases with decreasing chain length. The enhancement of k_p seen with decreasing chain length or increasing ν_{rep} is 25%, which is close to the value seen in k_p from CLDs without broadening. The extent of k_p variation with chain length derived from both types of CLD in the present work is comparable to the enhancement reported for experimental data in the literature.[11] As will be discussed in a subsequent section, the shape of the k_p-L curves in ref 11 is significantly different from that seen in this work.

This demonstrates that it is extremely important to report not only k_p data derived from PLP−SEC but also all experimental details for individual experiments.

Variation of c_R^0 at Constant Laser Pulse Repetition Rate. The CLDs considered so far were all obtained applying a primary radical concentration c_R^0 of 10^{-7} L mol^{-1} s^{-1}. Additional simulations were carried out for a wide range of c_R^0 values to determine the limiting laser pulse repetition rates that yield structured CLDs, allowing for the determination of k_p. Further, it will be tested how c_R^0 influences the variation of k_p with L_i.

For laser pulse repetition rates of 0.5 and 25 Hz, c_R^0 values ranging from 5×10^{-9} to 4×10^{-7} mol L^{-1} and from 1×10^{-7} to 1×10^{-5} mol L^{-1}, respectively, were introduced into the modeling. In all cases CLDs were obtained that exhibit at least one maximum at L_1 and a shoulder at around $2L_1$ in the derivative curve. The broadening procedure was applied to the CLDs with $\sigma_v b = 0.04$, and the associated derivative curves show fewer maxima. For both types of CLDs, k_p values were calculated from L_1. The results are summarized in Table 2. For 0.5 Hz no significant influence of c_R^0 on k_p is seen for $\sigma_v b = 0$. There is a slight decrease of about 5% in k_p for the higher values of c_R^0 for $\sigma_v b = 0.04$. In contrast, there is a distinct variation of k_p with c_R^0 for the higher repetition rate of 25 Hz. In going from 1×10^{-5} to 1×10^{-7} mol L^{-1}, k_p is increased by about 28%. If the value for 1×10^{-7} is skipped (only the first inflection point and a shoulder at around $2L_1$ are observed), an increase of about 15% is still detected. The variation in k_p is smaller for broadened CLDs.

These findings indicate that k_p determination at low repetition rate is insensitive to the primary radical concentration as long as a structured CLD is obtained with at least two inflection points and with L_2 approximately twice the value of L_1. In contrast, at high repetition rates and consequently low characteristic chain length L_1, the choice of the radical concentration c_R^0 strongly influences the position of the inflection points of the CLD and the k_p values, even though higher order inflection points occur that fulfill $L_2 \sim 2L_1$, $L_3 \sim 3L_1$. In general, the higher ν_{rep} introduced into the modeling, the higher is the value of c_R^0 required to generate CLDs that yield k_p values close to the theoretical value. This observation is consistent with the findings from ref 3. Thus, a strong dependence of k_p with ν_{rep} may be observed experimentally if a low radical concentration c_R^0 is chosen for the PLP experiment. Most experiments are carried out such that a solution of monomer and photoinitiator is prepared, and this solution is used for polymerizations with various laser pulse repetition rates. Even if structured CLDs are obtained for high values of ν_{rep}, the CLDs will cor-

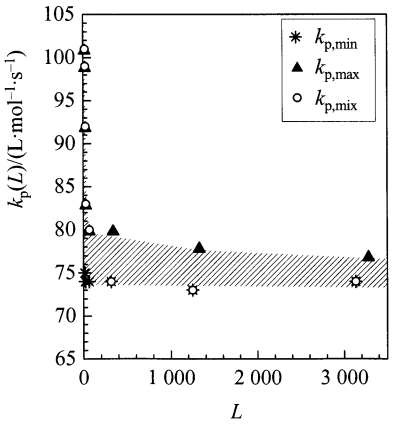

Figure 6. Propagation rate coefficients calculated from the first inflection point as a function of the corresponding chain length. Filled symbols represent $k_{p,max}$ and stars represent $k_{p,min}$ at each repetition rate applied. The open circles refer to $k_{p,mix}$. For details see text. The crisscrossed area between $k_{p,min}$ and $k_{p,max}$ values indicates the range of k_p values which may be derived at each chain length if c_R^0 is chosen accordingly.

Table 3. Minimum and Maximum Values for L_i and k_{pi} Derived from the First and Second Point of Inflection, Respectively, for Various Laser Pulse Repetition Rates ν_{Rep}; For Details See Text

ν_{rep}/Hz	$L_{1,min}$	$k_{p1,min}$ / L mol^{-1} s^{-1}	$L_{1,max}$	$k_{p1,max}$/ L mol^{-1} s^{-1}	k_p increase / %
0.2	3133	74	3281	77	4.1
0.5	1250	73	1327	78	6.8
2	316	74	339	80	8.1
10	63	74	68	80	8.1
25	25	74	28	83	12
33	19	74	24	92	24
40	16	75	21	99	32
50	13	75	17	101	35

respond to the low c_R^0 limit or the so-called low termination rate limit LTRL.[2] As shown by the modeling results in Table 1, this will most probably result in a k_p value that is enhanced at the higher laser pulse repetition rate.

In addition to ν_{rep} of 0.5 and 25 Hz, CLDs were modeled for further values of ν_{rep} with a wide range of c_R^0 values. By this method, for each ν_{rep} the highest and lowest value of c_R^0 were found that yield a CLD with a first and second inflection point. CLDs obtained for the low c_R^0 values refer to the low termination rate limit LTRL and CLDs for the highest c_R^0 values to the high termination rate limit HTRL. For all of these CLDs k_p values have been calculated. For each ν_{rep} the smallest k_p, $k_{p,min}$, and the highest k_p, $k_{p,max}$, calculated from the first inflection point are listed in Table 3. As expected, in general the differences between $k_{p,min}$ and $k_{p,max}$ are only small for low repetition rates, whereas at higher ν_{rep}, k_p changes by up to 35%. The results show that the observed variation of k_p with laser pulse repetition rate depends on the radical concentration of the individual experiments. Figure 6 presents $k_{p,min}$ and $k_{p,max}$ as a function of chain length. It demonstrates that $k_{p,max}$ varies significantly with L, whereas $k_{p,min}$ is almost constant. The crisscrossed area between $k_{p,min}$ and $k_{p,max}$ indicates the range of k_p values that may be derived for various ν_{rep} and c_R^0.

Considering experiments directed toward the determination of k_p values, most probably for a number of ν_{rep} the derived k_p is close to $k_{p,min}$ and for some ν_{rep} close to $k_{p,max}$. If it is assumed that experiments are carried

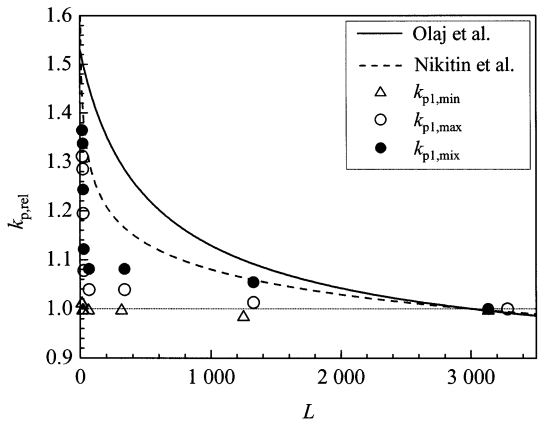

Figure 7. Variation of k_p with chain length on a relative scale; open symbols refer to $k_{p1,min}$ and $k_{p1,max}$ as indicated; filled symbols, $k_{p,mix}$ derived in this work; full line, $k_p(L)$ according to ref 11; dashed line, $k_p(L)$ according to ref 19.

out with similar initiator concentrations, generally at high ν_{rep} CLDs typical for the LTRL, and thus k_p values close to $k_{p,max}$ will be obtained. In contrast, at low ν_{rep} CLDs of the HTRL type and thus k_p values close to $k_{p,min}$ are derived. The situation is imitated by considering a mixture of $k_{p,min}$ and $k_{p,max}$, represented by $k_{p,mix}$, from Table 3 as a function of L_1. For ν_{rep} of 0.5, 0.2, and 2 Hz $k_{p,min}$ is plotted; for the higher ν_{rep} values $k_{p,max}$ is plotted. The filled symbols representing $k_{p,mix}$ in Figure 6 indicate a strong variation of k_p with L_1, with k_p at low L_1 being 27% above k_p at high L_1. This strong increase of k_p is observed, although a constant k_p of 75 L mol^{-1} s^{-1} has been used in all calculations. Furthermore, the modeling is only based on reasonable kinetic coefficients and concentrations.

After showing that a significant variation of k_p with ν_{rep} is seen in the PREDICI simulations, too, it is interesting to compare this change with how k_p is influenced by L_1 as reported in the literature. As mentioned before, in ref 11 a strong influence of L_i on k_p was observed. The experimental results for styrene were fit according to the following equation (eq 6b in ref 11):

$$F(L) = f(0) - A + ABL^{-1} \ln[(B + L)/B] \qquad (2)$$

with $f(0) = 107.0$, $A = 47.4$, and $B = 256.3$ taken from Table 4 in ref 11. To compare the change of k_p with L calculated according to eq 2 with the simulation results from this work, relative values are considered. Thus, Figure 7 plots $F(L)/F(3000)$ as a function of L. The simulation results from this work are given relative to k_p determined for 0.2 Hz with L_1 being around 3000: $k_{p,min}/k_{p,min}(0.2\ Hz)$ and $k_{p,max}/k_{p,max}(0.2\ Hz)$. The $k_{p,mix}$ is given relative to $k_{p,min}(0.2\ Hz)$. Very recently, Nikitin et al.[19] used a power law expression to describe k_p values as a function of L (eq 3).

$$k_p = k_{p,0} L^{-0.07} \qquad (3)$$

Equation 3 was used to fit experimental and simulation results.

Again, relative k_p data given as $k_p/k_p(3000)$ are calculated and are contained in Figure 7. Figure 7 clearly shows that the variation of k_p with L observed by Olaj and co-workers[11] is the strongest. The variation of k_p extends up to chain lengths of almost 3000. The change of k_p with L calculated according to Nikitin at

al.[19] is less pronounced but is also seen up to chain length of almost 3000. In contrast, the $k_{p,min}$ and $k_{p,max}$ data derived in this work are significantly influenced only for chain lengths below 200. A slightly stronger variation is seen for $k_{p,mix}$, because the ratio of $k_{p,max}$ and $k_{p,min}$(0.2 Hz) is calculated, with $k_{p,min}$ generally being below $k_{p,max}$. The results obtained for $k_p(L)$ via modeling with PREDICI agree well with experimental k_p data for styrene bulk polymerizations, which were obtained for ν_{rep} varying between 0.33 and 50 Hz.[20] These experiments also indicate that k_p changes only slightly for chain length above 200. Only for high repetition rates and thus values of $L_1 < 200$ an increase of k_p by around 30% is seen.

Conclusions

The modeling work presented was carried out with a constant value of k_p, and the modeling is exclusively based on kinetic coefficients and concentrations. Thus, the modeling can show whether experimentally observed changes in k_p are necessarily due to a chain-length dependence of k_p. The modeling results indicate that, for identical values of k_p and c_M used in the simulations, strongly varying k_p values are derived. These changes are induced by a variation of ν_{rep} if the primary radical concentration c_R^0 is kept constant or due to a variation of c_R^0 if ν_{rep} is kept constant. Consequently, the experimental finding that observed k_p values increase with increasing ν_{rep} or with decreasing L_i is not necessarily due to a chain-length dependence of k_p. Just by the choice of the initiating radical concentration, variations in L_1 and thus in k_p may be seen or may disappear.[21] Of course, in addition to variations in k_p caused by the shape of the MWD or CLD, other factors may also contribute to the experimentally observed variation of k_p with chain length, e.g., such as the occurrence of local monomer concentrations.[11]

As a conclusion from the modeling results, it is very important to check experimental CLDs (or MWDs) not only with respect to the occurrence of at least two inflection points but also with respect to the invariance of k_p with initiating radical concentration.[4,6,22] The variation of c_R^0 may be achieved by changing the initiator concentration and/or the energy of the laser pulses. Further, c_R^0 should be changed significantly, at least by half an order of magnitude. The described procedure should be applicable to investigations into methacrylates or styrenes. In the case of acrylate or vinyl ester (e.g., vinyl acetate) polymerizations, it is fairly difficult to find suitable conditions for PLP due to the high rate coefficients for the chain-transfer reaction to monomer or due to the termination reaction. For these monomers often only a very narrow range of c_R^0 values will result in a PLP structured distribution. Then, only the occurrence of higher inflection points may be the consistency criterion which will be fulfilled. In these cases k_p values derived may not originate from the robust regime where k_p is independent of L_1, and it must be checked carefully, e.g., by modeling of the MWDs, whether further conclusions may be drawn from the experimental results.

In general, experimentally derived k_p values will approach the true k_p as the chain length increases. The modeling results presented show that it is extremely important to report not only the k_p data derived from PLP−SEC experiments but also the experimental details for each individual experiment.

Acknowledgment. I thank Michael Buback for many interesting and stimulating discussions and Robin A. Hutchinson for providing helpful comments before publication.

References and Notes

(1) Olaj, O. F.; Bitai, I.; Hinkelmann, F. *Makromol. Chem.* **1987**, *188*, 1689. Olaj, O. F.; Schnöll-Bitai, I. *Eur. Polym. J.* **1989**, *25*, 635.
(2) Sarnecki, J.; Schweer, J. *Macromolecules* **1995**, *28*, 4080. Bandermann, F.; Günther, C.; Schweer, J. *Macromol. Chem. Phys.* **1996**, *197*, 1055.
(3) Buback, M.; Busch, M.; Lämmel, R. A. *Macromol. Theory Simul.* **1996**, *5*, 845.
(4) Beuermann, S.; Buback, M.; Davis, T. P.; Gilbert, R. G.; Hutchinson, R. A.; Olaj, O. F.; Russell, G. T.; Schweer, J.; van Herk, A. M. *Macromol. Chem. Phys.* **1997**, *198*, 1545.
(5) Beuermann, S.; Buback, M.; Davis, T. P.; Gilbert, R. G.; Hutchinson, R. A.; Kajiwara, A.; Klumperman, B.; Russell, G. T. *Macromol. Chem. Phys.* **2000**, *201*, 1355.
(6) Buback, M.; Gilbert, R. G.; Hutchinson, R. A.; Klumperman, B.; Kuchta, F.-D.; Manders, B. G.; O'Driscoll, K. F.; Russell, G. T.; Schweer, J. *Macromol. Chem. Phys.* **1995**, *196*, 3267.
(7) Brandrup, A., Immergut, E. H., Eds.; *Polymer Handbook*, 3rd ed.; Wiley: New York, 1989.
(8) van Herk, A. M. *Macromol. Theory Simul.* **2000**, *9*, 433.
(9) Beuermann, S.; Buback, M. *Prog. Polym. Sci.* **2002**, *27*, 191.
(10) See for example: Hutchinson, R. A.; Beuermann, S.; Paquet, D. A., Jr.; McMinn, J. H.; Jackson, C. *Macromolecules* **1998**, *31*, 1542.
(11) Olaj, O. F.; Vana, P.; Zoder, M.; Kornherr, A.; Zifferer, G. *Macromol. Rapid Commun.* **2000**, *212*, 913.
(12) Olaj, O. F.; Vana, P.; Zoder, M. *Macromolecules* **2002**, *35*, 1208.
(13) Moad, G.; Solomon, D. H. *The Chemistry of Free Radical Polymerization*; Pergamon: Oxford, 1995.
(14) Odian, G. *Principles of Polymerization*, 2nd ed.; Wiley: New York, 1981.
(15) Gridnev, A. A.; Ittel, S. D. *Macromolecules* **1996**, *29*, 5864.
(16) Moad, G.; Rizzardo, E.; Solomon, D. H.; Beckwith, A. L. J. *Polym. Bull. (Berlin)* **1992**, *29*, 647.
(17) Beuermann, S.; Paquet, Jr., D. A.; McMinn, J. H.; Hutchinson, R. A. *Macromolecules* **1996**, *29*, 4206.
(18) Hutchinson, R. A.; Richards, J. R.; Aronson, M. T. *Macromolecules* **1994**, *27*, 4530.
(19) Nikitin, A. N.; Evseev, A. V.; Buback, M.; Feldermann, A.; Jürgens, M.; Nelke, D. *Macromol. Theory Simul.*, submitted.
(20) Beuermann, S.; Buback, M. Manuscript in preparation.
(21) Recently, Vana et al. also mentioned the importance of chosing proper experimental conditions for obtaining well-structured molecular weight distributions: Vana, P.; Lachlan, H. Y.; Davis, T. P. *Macromolecules* **2002**, *35*, 3008.
(22) Ganachaud, F.; Balic, R.; Monteiro, M. J.; Gilbert, R. G. *Macromolecules* **2000**, *33*, 8589.

MA020437M